EPJ Web of Conferences **60**, 20014 (2013)
DOI: 10.1051/epjconf/20136020014

Measurement of the WW Production Cross Section in Proton-Proton Collisions with the ATLAS Detector

Jiří Hejbal[1,a] on behalf of the ATLAS Collaboration.

[1] *Institute of Physics, Academy of Sciences of the Czech Republic, Praha, Czech Republic*

Abstract. Measurements of the W^+W^- production using the leptonic decay channels are analysed using data collected by the ATLAS detector at the CERN Large Hadron Collider. The precise measurement of W+W- production is important for comparing to the Standard Model expectation, and also provides a detailed understanding of this process as a background in searches for new physics phenomena.

1 Introduction

Measurements of vector boson pair production at particle colliders provide important tests of the electroweak sector of the Standard Model (SM). Vector boson pair production at the Large Hadron Collider [1] (LHC) also represents an important source of background to Higgs boson production and to searches for physics beyond the SM. Diboson processes also provide new constraints on Triple Gauge Couplings. The latest ATLAS results on WW production are presented using data collected at centre-of-mass energy of 7 TeV.

2 ATLAS detector

The ATLAS detector [2] consists of an inner tracking system (inner detector, or ID) surrounded by a superconducting solenoid providing a 2 T magnetic field, electromagnetic and hadronic calorimeters, and a muon spectrometer (MS) incorporating three large superconducting toroid magnets arranged with an eight-fold azimuthal coil symmetry around the calorimeters. The ID consists of silicon pixel and microstrip detectors, surrounded by a transition radiation tracker. The electromagnetic calorimeter is a lead/liquid-argon (LAr) detector. Hadron calorimetry is based on two different detector technologies, with scintillator tiles or LAr as active media, and with either steel, copper, or tungsten as the absorber material. The MS comprises three layers of chambers for the trigger and for track measurements.

3 SM WW production

We present a measurement of W^+W^- inclusive and differential production cross sections in pp collisions and limits on anomalous WWZ and $WW\gamma$ triple gauge couplings (TGCs) in purely leptonic decay channels $WW \to \ell\nu\ell'\nu'$ with $\ell,\ell' = e,\mu$. Processes with τ leptons decaying into electrons or muons with additional neutrinos are also included. Three final states are considered based on the lepton flavor, namely $e^+e^-E_T^{miss}$, $\mu^+\mu^-E_T^{miss}$ and $e^\pm\mu^\mp E_T^{miss}$.

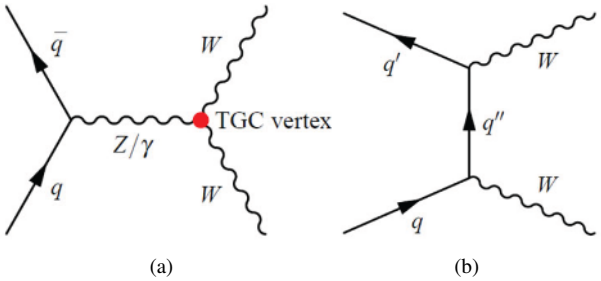

Figure 1. SM LO Feynman diagrams for WW production through the $q\bar{q}$ initial state at the LHC for (a) the s-channel and (b) the t-channel [3].

Leading-order (LO) Feynman diagrams for WW production at the LHC include s-channel production with either a Z boson or a virtual photon as the mediating particle or u- and t-channel quark exchange. The s- and t-channel diagrams are shown in Fig. 1.

Gluon-gluon fusion processes contribute a background of about 3% to the total cross section [3]. The processes involving SM Higgs Boson production ($\approx$ 3% for Higgs mass of 126 GeV), vector boson fusion (VBF) and double parton scattering (DPS) are not considered in estimating the contribution of background processes.

4 Event selection

After applyping data quality requirements and selection criteria for electrons, muons, jets and vertices [3], the events are dominated by Drell-Yan processes. To reject these background contributions, different requirements are applied to each final state. The variables used are the dilep-

[a] e-mail: jiri.hejbal@cern.ch

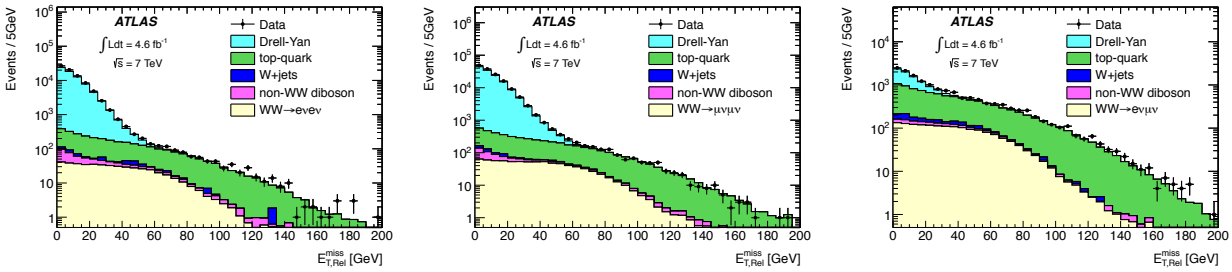

Figure 2. Comparison between data and predictions of various generators at detector level for the $E_{\mathrm{T,\,Rel}}^{\mathrm{miss}}$ distribution before the $E_{\mathrm{T,\,Rel}}^{\mathrm{miss}}$ cut for the ee, $\mu\mu$ and $e\mu$ channels, respectively [3].

ton invariant mass $m_{\ell\ell'}$ and a modified missing transverse energy, $E_{\mathrm{T,\,Rel}}^{\mathrm{miss}}$, definied as:

$$E_{\mathrm{T,\,Rel}}^{\mathrm{miss}} = \begin{cases} E_{\mathrm{T}}^{\mathrm{miss}} \times \sin(\Delta\phi) & \text{if } \Delta\phi < \pi/2 \\ E_{\mathrm{T}}^{\mathrm{miss}} & \text{if } \Delta\phi \geq \pi/2, \end{cases} \quad (1)$$

where $\Delta\phi$ is the difference in the azimuthal angle between the $\vec{E}_{\mathrm{T}}^{\mathrm{miss}}$ and the nearest lepton or jet.

The $E_{\mathrm{T,\,Rel}}^{\mathrm{miss}}$ variable is designed to reject events where the apparent $E_{\mathrm{T}}^{\mathrm{miss}}$ arises from a mismeasurement of lepton momentum or jet energy. The selection criteria applied to $m_{\ell\ell'}$ and $E_{\mathrm{T,\,Rel}}^{\mathrm{miss}}$ are:

- $m_{\ell\ell'} > 15, 15, 10$ GeV, $|m_{\ell\ell'} - m_Z| > 15, 15, 0$ GeV
- $E_{\mathrm{T,\,Rel}}^{\mathrm{miss}} > 45, 45, 25$ GeV

for the ee, $\mu\mu$ and $e\mu$ channels, respectively. With the application of the $m_{\ell\ell'}$ and $E_{\mathrm{T,\,Rel}}^{\mathrm{miss}}$ selection criteria, the remaining background events come mainly from $t\bar{t}$ and single top-quark processes. To reject this background contribution, events are vetoed if there is at least one jet candidate with $p_{\mathrm{T}} > 25$ GeV and $|\eta| < 4.5$. To further reduce the Drell-Yan contribution, the transverse momentum of the dilepton system, $p_{\mathrm{T}}(\ell\ell')$, is required to be greater than 30 GeV for all three channels.

For illustration, Figure 2 shows comparison between data and predictions of the MC generators at detector level for the $E_{\mathrm{T,\,Rel}}^{\mathrm{miss}}$ distribution before the $E_{\mathrm{T,\,Rel}}^{\mathrm{miss}}$ cut is applied to the ee, $\mu\mu$ and $e\mu$ channels, respectively.

5 Cross sections

The WW cross section is measured in the fiducial phase space and extrapolated to the total phase space. The fiducial phase space is defined at the particle level by selection criteria similar to those used at detector level and includes the jet veto as well. The fiducial cross section for the $pp \to WW + X \to \ell\nu\ell'\nu' + X$ process is calculated using:

$$\sigma_{WW}^{\mathrm{fid}} = \frac{N_{\mathrm{data}} - N_{\mathrm{bkg}}}{C_{WW} \times \mathcal{L}} \quad (2)$$

where N_{data} and N_{bkg} are numbers of observed data events and estimated background events, respectively. C_{WW} is defined as the ratio of the number of events satisfying all selection criteria at detector level to the number of events

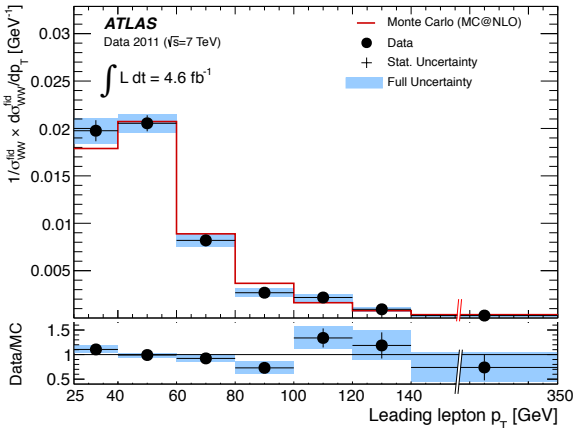

Figure 3. The normalized differential WW cross section for data corrected for detector effects as a function of the leading lepton p_{T} compared to the SM prediction [3].

produced in the fiducial phase space and is estimated from simulations. $\mathcal{L}$ is the integrated luminosity of the data sample.

The total cross section σ_{WW} for the inclusive $pp \to WW + X$ process is calculated for each channel using:

$$\sigma_{WW} = \frac{N_{\mathrm{data}} - N_{\mathrm{bkg}}}{C_{WW} \times A_{WW} \times \mathrm{BR} \times \mathcal{L}} \quad (3)$$

where A_{WW} represents the kinematic and geometric acceptance from the total phase space to the fiducial phase space, and BR is the branching ratio for both W bosons decaying into $e\nu$ or $\mu\nu$ (including decays through τ leptons with additional neutrinos).

To obtain the normalized differential WW cross section in the fiducial phase space ($1/\sigma_{WW}^{\mathrm{fid}} \times d\sigma_{WW}^{\mathrm{fid}}/dp_{\mathrm{T}}$), the reconstructed leading lepton p_{T} distribution is corrected for detector effects after the subtraction of background contamination and unfolded to the particle level. The resulting normalized fiducial cross sections extracted in bins of the leading lepton p_{T} together with the SM predictions is shown in Fig. 3.

6 Signal and background yields

The number of events selected in data and the estimated background contributions for the three individual chan-

Table 1. Summary of observed and expected numbers of signal and background events in three individual channels and their combination [3].

	ee	$\mu\mu$	$e\mu$	Combined
Data	174	330	821	1325
WW	100	186	538	824
Top	22	32	87	141
W+jets	21	7	70	98
Drell-Yan	12	34	5	51
Other dibosons	13	21	44	78
Total background	68	94	206	369
Total expected	169	280	744	1192

nels and the combined channel is summarized in Table 1. The expected numbers of WW signal events for the individual and the combined channels are also shown. In total 1325 $\ell\ell' + E_{\mathrm{T}}^{\mathrm{miss}}$ candidates are observed in data with 824 ± 4 (stat) $\pm$ 69 (syst) signal events expected from the WW process and $369 \pm$ 31 (stat) $\pm$ 53 (syst) background events expected from non-WW processes.

7 Background

The processes producing the $\ell\ell' + E_{\mathrm{T}}^{\mathrm{miss}}$ signature with no reconstructed jets in the final state are Z+jet (Drell-Yan background) when apparent $E_{\mathrm{T}}^{\mathrm{miss}}$ is generated from the mismeasurement of the p_{T} of the two leptons from Z boson decay; top-quark production when b-jets are not reconstructed or identified (top-quark background); W+jet production when a jet is misidentified as a lepton (W+jets background); W+γ production with photon identified as an electron; $W + \gamma^*$ when one lepton is not detected; $WZ \rightarrow lll\nu$ where one lepton not detected; $ZZ \rightarrow ll\nu\nu$ where invariant mass is not near the Z-mass. The contribution from QCD multijet production when two jets are reconstructed as leptons is found to be negligible.

8 Extracted TGC Limits

The reconstructed leading lepton p_{T} distribution is also used to set limits on anomalous WWZ and $WW\gamma$ TGCs. The Lorentz invariant Lagrangian describing the WWZ and $WW\gamma$ interactions has 14 independent coupling parameters. Assuming electromagnetic gauge invariance and C and P conservation, the number of independent parameters reduces to five: g_1^Z, κ_Z, κ_γ, λ_Z and λ_γ. Each of the couplings is usually modified by a factor depending on scale Λ with the general form $\alpha(\hat{s}) = \alpha_0/(1 + \hat{s}/\Lambda^2)^2$, where α_0 is the coupling value at low energy and $\sqrt{\hat{s}}$ is the invariant mass of the WW pair.

In the SM, the coupling parameters have the following values: $g_1^Z = \kappa_Z = \kappa_\gamma = 1$ and $\lambda_Z = \lambda_\gamma = 0$. Limits in the LEP scenario, where we assume $\Delta\kappa_\gamma = (\cos^2\theta_W/\sin^2\theta_W)(\Delta g_1^Z - \Delta\kappa_Z)$, and $\lambda_Z = \lambda_\gamma$ are compared with limits obtained from the CMS [4], CDF [5], DØ [5] and LEP [6] experiments in Fig. 4.

Table 2 shows expected and observed 95% confidence level limits on anomalous WWZ and $WW\gamma$ couplings in the Equal Couplings scenario for QCD scale $\Lambda = 6$ TeV. In this scenario we assume that the WWZ and $WW\gamma$ couplings are equal ($\Delta\kappa_Z = \Delta\kappa_\gamma$, $\lambda_Z = \lambda_\gamma$, and $g_1^Z = 1$).

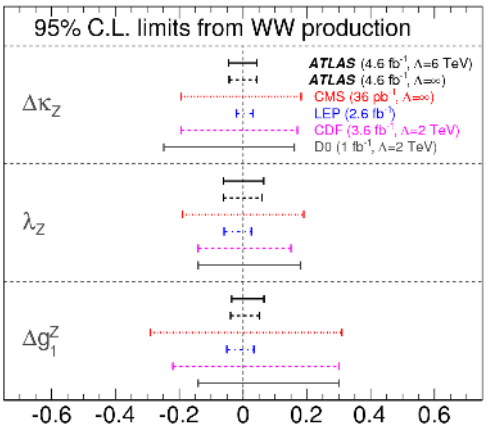

Figure 4. Comparison of anomalous TGC limits from ATLAS, CMS, CDF, DØ and LEP experiments for the LEP scenario [3].

Table 2. The expected and observed limits on anomalous TGCs in Equal Couplings scenario for QCD scale $\Lambda = 6$ TeV [3].

Parameter	Expected	Observed
$\Delta\kappa_Z$	$[-0.058, 0.089]$	$[-0.061, 0.093]$
$\lambda_Z = \lambda_\gamma$	$[-0.060, 0.062]$	$[-0.062, 0.065]$

9 Summary and results

The WW inclusive production cross section in proton-proton collisions at $\sqrt{s} = 7$ TeV is measured using 4.6 fb^{-1} of data collected with the ATLAS detector at the LHC. In total 1325 candidates are selected with an estimated background of 369 ± 61 events channels into ee, $\mu\mu$ and $e\mu$ final states.

The combined production cross section $\sigma(pp \rightarrow WW + X)$ 51.9 $\pm$ 2.0 (stat) $\pm$ 3.9 (syst) $\pm$ 2.0 (lumi) pb, compatible with the SM NLO prediction of $44.7^{+2.1}_{-1.9}$ pb.

References

[1] L. Evans and P. Bryant 2008 JINST 3 S08001.
[2] ATLAS Collaboration, 2008 JINST 3 S08003.
[3] ATLAS Collaboration, Phys. Rev. D **87**, 112001 (2013).
[4] CMS Collaboration, Phys. Lett. B **699**, 25 (2011).
[5] CDF Collaboration, Phys. Rev. Lett. **104**, 201801 (2010); D0 Collaboration, Phys. Rev. Lett. **103**, 191801 (2009); *ibid.*, Phys. Rev. D **80**, 053012 (2009).
[6] ALEPH Collaboration, Phys. Lett. B **614**, 7 (2005); DELPHI Collaboration, Eur. Phys. J. C **54**, 345 (2008); L3 Collaboration, Phys. Lett. B **586**, 151 (2004); OPAL Collaboration, Eur. Phys. J. C **33**, 463 (2004).